ELSEVIER

Physica C 296 (1998) 269–280

PHYSICA C

Superconductivity of a striped phase at the atomic limit

Antonio Bianconi *, Antonio Valletta, Andrea Perali, Naurang L. Saini

Dipartimento di Fisica and INFM, Università di Roma 'La Sapienza', P. Aldo Moro 5, I-00185 Roma, Italy

Received 9 September 1997; accepted 27 October 1997

Abstract

The resonant amplification of the superconducting critical temperature, the isotope effect, the change of the chemical potential in a particular 2D striped phase formed by superconducting stripes of width L alternated by separating stripes of width W with a period λ_p at the atomic limit is studied. The critical temperature shows a 'shape resonance' by tuning the charge density where the chemical potential μ is in the range $E_n < \mu < E_n + \hbar\omega_0$, where E_n is the bottom of the nth superlattice subband for $n > 2$, and $\hbar\omega_0$ is the energy cutoff for the pairing interaction. The maximum critical superconducting temperature is reached at the cross-over from 2D to 1D behavior. The particular properties of this electronic phase and its similarities with the normal and superconducting properties of doped cuprate perovskites are discussed. © 1998 Elsevier Science B.V.

Keywords: T_c amplification; Superlattice of quantum wires; Superconductivity; Heterostructures at the atomic limit

1. Introduction

Superconductivity in doped cuprate perovskites has been discovered in 1986 looking for a material with a large electron–lattice interaction given by a dynamic Jahn Teller interaction [1]. Four years later it was found that these materials are heterostructures made of superconducting CuO_2 films (S) intercalated with insulating or normal metallic layers (I, or M) [2–6], forming a superlattice (SISISI; or SMSMSM) of Josephson coupled layers [7,8]. Moreover, the CuO_2 plane of the high-T_c superconductors has been found to be inhomogeneous and it is now becoming more generally recognized that the anomalous transport properties of the CuO_2 plane may be due to a dynamic phase segregation in which the system condense into large stripe domains [9–17].

Some experiments have shown the coexistence of itinerant charges with an effective mass $m^* \sim 2.5 \pm 0.5$ in units of the electron mass and b_1 ($d_{x^2-y^2}$) symmetry and more localized charges (or polarons) having a mixed b_1 and a_1 ($3d_{r^2-z^2}$) symmetry from a pseudo Jahn Teller interaction. The localized charges are associated with a rhombic distortion of the CuO_4 square plane, a displacement of Cu out of the plane and a shortening of the Cu–O(apical) distance [18–22]. The ordering of the polarons forming linear arrays of distorted Cu sites in the

* Corresponding author. Fax: +39 6 495 7697; E-mail: antonio.bianconi@roma1.infn.it.

PII S0921-4534(97)01825-X

CuO_2 plane was found in 1990 [18] and confirmed by many experiments using the joint analysis of X-ray absorption (XAS) and diffraction (XRD) [12].

These data have shown the coexistence in the superconducting phase of:

1. polarons ordered in a one-dimensional incommensurate charge density wave (1D ICDW), and
2. itinerant charges with strong Coulomb and magnetic interactions.

The two types of charge carriers are segregated in different spatial domains formed by alternated stripes of distorted (D-stripes) and undistorted (U-stripes) lattice. This phase segregation occurs as a function of the charge density at $T = 0$ K in a narrow range of charge density at a cross over region of metal–insulator transition (MIT) [23–26] and as a function of temperature below a characteristic temperature T^* characterized by the opening of a pseudogap on the Fermi surface.

In the insulating region, at low doping $\delta < 0.06$ holes per Cu site, the polarons get ordered in short and randomly distributed linear domain walls in an antiferromagnetic lattice [27]. In the metallic phase, at high doping levels, a homogeneous metal is formed. A similar charge segregation of 3D metallic ferromagnetic domains separated by insulating domains of Jahn Teller distorted lattice has been found near the metal insulator transition (MIT) in manganites exhibiting the colossal magnetoresistance effect [9,28,29].

The self-organization of polaron charges in the CuO_2 lattice forms a natural superlattice made of metallic quantum wires (U-stripes) alternated by D-stripes that play the role of spacers as shown in Fig. 1. In $Bi_2Sr_2CaCu_2O_{8+\delta}$ and $La_2CuO_{4+\delta}$ at optimum doping these lattice fluctuations with a short coherence length have been found to be pinned to the ordered interstitial oxygen inserted as dopants in the rocksalt layers [10–15] as shown by anomalous X-ray diffraction [12]. In the underdoped regime and in other systems, such as $La_{2-x}Sr_xCuO_4$, the randomly distributed dopants, the short coherence length and the slow dynamics of the 1D ICDW have masked the striped phase for a long time; however, they have been detected recently by fast probes such as EXAFS [16]. These lattice fluctuations are slower than the characteristic time scale for the electron pairing mechanism so that we can assume that the itinerant charge carriers are moving in a static superlattice of quantum stripes and the stripes of localized charges can be considered simply as a source for a 1D potential barrier for the itinerant carriers.

Measurements of the stripe width L and superlattice period by structural probes and of the wavevector k_F of the electrons at the Fermi surface by angular resolved photoemission have shown that the chemical potential is self-tuned near the bottom of the third superlattice subband ($k_F \sim k_3 \sim 3\pi/L$) where the density of states has a maximum (i.e. near the $n = 3$ shape resonance) [10–14]. This resonance provides not only a possible mechanism for understanding the amplification of the critical temperature from the low to the high temperature range in cuprate superconductors but also a direction to realize the synthesis of new superconductors with high critical temperature made of particular heterostructures of metallic stripes at the atomic limit. In these superlattices the stripe structure and the charge density are such that the chemical potential μ is tuned in the range $E_n < \mu < E_n + \hbar\omega_0$, where E_n is the bottom of the $n \geq 2$ superlattice subband and $\hbar\omega_0$ is the energy cutoff for the pairing interaction [30–32].

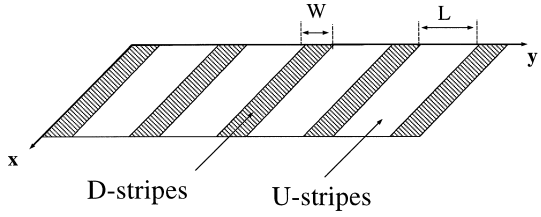

Fig. 1. A particular heterostructure made of metallic quantum stripes of width L (U-stripes) separated by stripes of width W (D-stripes) with a period $\lambda_p = W + L$.

This resonance can be realized by changing the stripe width and superlattice period for a fixed charge density (the energy E_n is controlled by the stripe structure) or in an equivalent way by changing the charge density, keeping fixed the stripe structure (the chemical potential μ is controlled by the charge density).

In this paper we report the calculations of the electronic properties for a simple free electron model in a superlattice of quantum stripes. This simple model is used to study the superconducting and related characteristics of this superlattice. We consider a 2D free electron gas with an electron number surface density $\rho = 5.8 \times 10^{14}$ cm^{-2} confined in a superlattice designed to tune the chemical potential near the bottom of 3rd subband, to keep the lateral superlattice dispersion to be of the order of $\sim \hbar\omega_0$ assuming an interaction cutoff $\hbar\omega_0 \sim 500$ K in agreement with experimental data for the cuprates. We find that the resonance in the superconducting critical temperature T_c occurs in a narrow charge density range having similar width and anisotropic shape as in cuprate superconductors. We have calculated the isotope coefficient (α) for this particular striped phase and we have reproduced the experimentally observed anomalous doping dependence of α in cuprates [33–35]. Finally, we show that, going from one side of the resonance (overdoped regime) to the other (underdoped regime), a partial gap, or pseudogap, opens at a particular point of the Fermi surface that agrees qualitatively with recent angular resolved photoemission experiments [36–40].

2. The Fermi surface and the density of states

We consider a free electron gas with an effective mass m^* moving in a superlattice of quantum stripes of width L separated by a periodic potential barrier $V(x,y)$ of amplitude V_b and width W along the y-direction and constant in the x-direction

$$V(y) = -V_b \sum_{m=-\infty}^{\infty} \theta\left(\frac{W}{2} - |m\lambda_p - y|\right). \tag{1}$$

The solution of the Schrödinger equation for this system is given as:

$$\psi_{n,k_x,k_y}(x,y) = e^{ik_x x} \cdot e^{ik_y q\lambda_p} \psi_{n,k_y}(y), \tag{2}$$

where

$$\psi_{n,k_y}(y) = \alpha e^{ik_w \tilde{y}} + \beta e^{-ik_w \tilde{y}}, \quad \text{for } |\tilde{y}| < L/2;$$

$$\psi_{n,k_y}(y) = \gamma e^{ik_b \tilde{y}} + \delta e^{-ik_b \tilde{y}}, \quad \text{for } |\tilde{y}| \geq L/2;$$

$$\tilde{y} = y - \lambda_p q; \quad q = \text{Integer part of} \left[\frac{y}{\lambda_p}\right]; \quad \hat{y} = y - \lambda_p q - \frac{\lambda_p}{2}.$$

The coefficients α, β, γ and δ are obtained by imposing the Bloch conditions with periodicity λ_p, the continuity conditions of the wave function and its derivative at $L/2$, and finally by normalization in the surface unit.

The solution of the eigenvalue equation for E gives the electronic energy dispersion for the n subbands with energy $\varepsilon_n(k_x,k_y) = \varepsilon(k_x) + E_n(k_y)$, where $\varepsilon(k_x) = (\hbar^2/2m)k_x^2$ is the free electron energy dispersion in the x-direction and $E_n(k_y)$ is the dispersion in the y-direction. We have derived N_b solutions for $E_n(k_y)$ $(1 \leq n \leq N_b)$ for each k_y in the Brillouin zone of the superlattice giving dispersion in the y-direction of the first N_b subbands with $k_x = 0$.

We present here the results of the calculations for a particular superlattice with stripes of width $L = 10.5$ Å alternated by separating stripes of width $W = 5$ Å with a superlattice period of $\lambda_p = 15.5$ Å. The potential barrier is fixed at $V_b = 1.3$ eV and the effective mass of electrons $m^* = 2.5$. The density of states (DOS) and

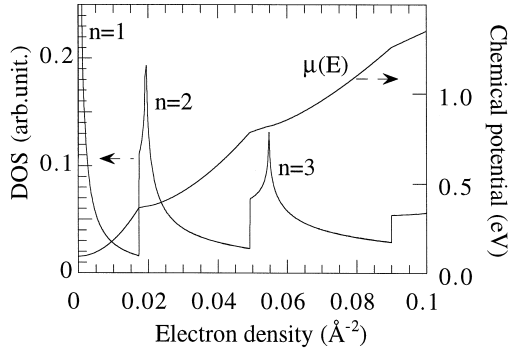

Fig. 2. The density of states (DOS) as a function of the electron charge density and chemical potential. The peaks corresponding to the first ($n=1$), second ($n=2$), and third ($n=3$) subbands are shown.

the chemical potential as a function of the charge density is shown in Fig. 2. The first ($n=1$) and second ($n=2$) subbands are nearly one-dimensional (1D); the third subband is dispersing in the transverse y-direction from its energy bottom E_3 at $k_y = 2\pi/\lambda_p$ and $k_x = 0$ to its energy top E_c at $k_y = 3\pi/\lambda_p$, showing a total dispersion in the transverse direction, $\Delta E_{3\perp}$, forming a quasi two dimensional (2D) subband.

We have plotted in Fig. 3 the Fermi surface for the chemical potential in the range $E_3 < \mu < E_c$ and in the range $\mu > E_c$. The periodic 1D potential barrier breaks the closed circular Fermi surface for an homogeneous plane into broken segments. The first and the second subbands give origin to four segments in the range $0 < k_y < \pm\pi/\lambda_p$ and $\pm\pi/\lambda_p < k_y < \pm 2\pi/\lambda_p$ respectively. Two segments due to the third subband appear where the chemical potential is in the range $E_3 < \mu < E_c$ (or the charge density in the range $\rho_3 < \rho < \rho_c$) near

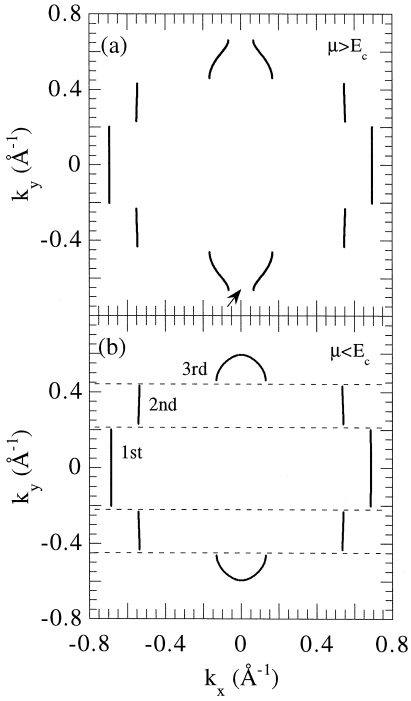

Fig. 3. The Fermi surface for the chemical potential (μ) above the critical energy E_c (panel a) and $\mu < E_c$ (panel b). The arrows indicate the opening of the pseudogap at E_c in the third subband.

$k_x \sim 0$, for $\pm 2\pi/\lambda_p < k_y < \pm 3\pi/\lambda_p$ that become longer with increasing charge density. These segments are broken at $k_x = 0$ and form 4 segments for $\rho > \rho_c$ or $\mu > E_c$ showing a pseudogap at $k_x = 0$. This result shows the opening of the pseudogap in the third subband going from the regime $E_3 < \mu < E_c$ or for the charge density in the range $\rho_3 < \rho < \rho_c$ (called hereafter overdoped regime) to the underdoped regime for $\mu > E_c$ or for $\rho > \rho_c$ (called hereafter underdoped regime).

The DOS for the chemical potential tuned near the bottom of the third subband is shown in Fig. 4(a). It shows a sharp step increase at the bottom of the third subband E_3 (corresponding to the charge density $\rho_3 \sim 0.051$ Å^{-2}) and a peak at the energy E_c (corresponding to the charge density ρ_c). The jump at ρ_3 is determined by the threshold of the contribution of the partial density of states of the third subband to the total density of states where the chemical potential is tuned above the bottom of the third subband E_3. The peak at ρ_c is due to an anisotropic Van Hove singularity where the chemical potential reaches the energy E_c at the top of the dispersion of the 3rd superlattice band in the y direction. The total energy dispersion of the 3rd subband $\Delta E_{3\perp}$ in the transverse direction determines the separation between the peak and the step edge. Where the chemical potential is tuned in the range $E_3 < \mu < E_c$ and the density in the range $\rho_3 < \rho < \rho_c$ (overdoped regime) the DOS shows a quasi 2D behavior while $\mu > E_c$ or for $\rho > \rho_c$ (underdoped regime) a 1D-like behavior dominates giving a DOS divergence of the type $(1/\varepsilon)^{1/2}$ as for a single stripe with infinite potential barrier $V_b \to \infty$.

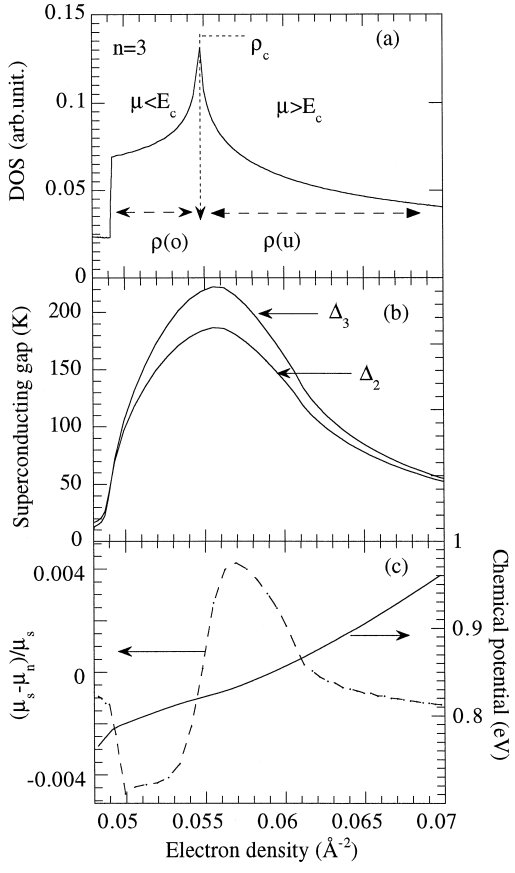

Fig. 4. (a) Density of states in the third subband. (b) The superconducting gaps in segments of the Fermi surface due to the second subband Δ_2 and that due to the third subband Δ_3 with the chemical potential tuned around the $n = 3$ "shape resonance". (c) The chemical potential and its variation going from the normal to the superconducting phase.

3. The resonance of the critical temperature

The calculation of the superconducting gap at $T = 0$ K is carried out using the BCS approach. We have solved the BCS equations for the gap as a function of the chemical potential in a self consistent manner. A generic cutoff energy $\hbar\omega_0$ for the effective pairing interaction of any magnetic, charge or phononic nature has been considered. The coupling term has been calculated taking into account the interference effects between the wave functions of the pairing electrons in the different subbands

$$V_{nn'}(k,k') = V_{n,k_y;n',k'_y}\theta\left(\hbar\omega_0 - |\varepsilon_n(k_x,k_y) - \mu|\right)\theta\left(\hbar\omega_0 - |\varepsilon_{n'}(k_{x'},k_{y'}) - \mu|\right), \tag{3}$$

where

$$V_{n,k_y;n',k'_y} = -V_0\int_S \mathrm{d}x\,\mathrm{d}y\,\psi^*_{n,-k_y}(y)\,\psi^*_{n,k_y}(y)\,\psi_{n',-k'_y}(y)\,\psi_{n',k'_y}(y) = -V_0\int_S \mathrm{d}x\,\mathrm{d}y\,|\psi_{n,k_y}(y)|^2|\psi_{n',k'_y}(y)|^2, \tag{4}$$

with $V_0 = \lambda/N_0$, where $N_0 = (1/4\pi)(2m/\hbar^2)$ is the 2D free electron density of states and λ is the effective coupling parameter for the ideal homogeneous material ($V_b = 0$); n and n' are the subband indexes. k_x ($k_{x'}$) is the component of the wavevector in the stripe direction (or longitudinal direction) and k_y, ($k_{y'}$) is the superlattice wavevector (in the transverse direction) of the initial (final) state in the pairing process, and μ the chemical potential.

In the BCS approximation, i.e., a separable kernel, the gap parameter has the same energy cut off $\hbar\omega_0$ as the interaction. Therefore, it has a value $\Delta_n(k_y)$ around the Fermi surface in a range $\hbar\omega_0$ depending from the subband index and the superlattice wave vector k_y. The self consistent equation for the ground state energy gap $\Delta_n(k_y)$ is:

$$\Delta_n(\mu,k_y) = -\frac{1}{2N}\sum_{n'k'_yk'_x}\frac{V_{nn'}(k,k')\,\Delta_{n'}(k_{y'})}{\sqrt{\left(E_{n'}(k_{y'}) + \varepsilon_{k_{x'}} - \mu\right)^2 + \Delta^2_{n'}(k_{y'})}}, \tag{5}$$

where N is the total number of wavevectors. This equation has been solved iteratively, with the convergence criterion fixed for a relative gap variation less than 10^{-4}. We obtain an anisotropic gap strongly dependent on the subband index and dependent on the superlattice wavevector k_y.

The charge density ρ and the chemical potential in the superconducting phase are related by:

$$\begin{aligned}\rho &= \frac{1}{S}\sum_{n}^{N_b}\sum_{k_x,k_y}\left(1 - \frac{\varepsilon_n(k_x,k_y) - \mu}{\sqrt{\left(\varepsilon_n(k_x,k_y) - \mu\right)^2 + \Delta^2_{n,k_y}}}\right)\\ &= 2\frac{\Delta k_y}{2\pi}\sum_{n=1}^{N_b}\sum_{k_y=0}^{\pi/\lambda_p}\left[\int_0^{\varepsilon_{\min}}\mathrm{d}\varepsilon\frac{N(\varepsilon)}{L_x}2 + \int_{\varepsilon_{\min}}^{\varepsilon_{\max}}\mathrm{d}\varepsilon\frac{N(\varepsilon)}{L_x}\left(1 - \frac{E_n(k_y) + \varepsilon - \mu}{\sqrt{\left(E_n(k_y) + \varepsilon - \mu\right)^2 + \Delta^2_{n,k_y}}}\right)\right],\end{aligned} \tag{6}$$

where

$$\varepsilon_{\min} = \max\left[0, \mu - \hbar\omega_0 - E_n(k_y)\right]; \quad \varepsilon_{\max} = \max\left[0, \mu + \hbar\omega_0 - E_n(k_y)\right];$$

and

$$N(\varepsilon) = \frac{L_x}{2\pi}\left(\sqrt{\frac{\hbar^2}{2m}}\varepsilon\right)^{-1}$$

and N_b is the number of the occupied subbands; L_x and L_y are the size of the considered surface S; the increment in k_y is taken as $\Delta k_y = 2\pi/L_y$.

The superconducting gap shows a shape resonance when the chemical potential is tuned near the bottom of the $n=3$ subband. The structure in the interaction gives 3 different values for the gap Δ_n in the first $(n=1)$ that is close to value of the second $(n=2)$ and in the third $(n=3)$ subband giving a system with an anisotropic gap in the different segments of the Fermi surface. The resonance shows a maximum of the gaps at a critical charge density ρ_c. Fig. 4(b) shows the resonance for the gaps in the second Δ_2 and third Δ_3 subbands as a function of the electron number density where we have considered the case for $\lambda = 1/3$ and $\hbar\omega_0 = 500$ K. The peak of the resonance takes place where the chemical potential is tuned at E_c, i.e. at a divergence of the density of states. The critical charge density ρ_c for the $n=3$ resonance is controlled by the stripe width L and the superlattice period λ_p that have been chosen to reproduce the value observed in cuprate perovskites.

The width of the resonance in Fig. 4(b) is controlled by the interaction cut off $\hbar\omega_0$ and the superlattice dispersion in the y-direction $\Delta E_{3\perp}$. The finite dispersion $\Delta E_{3\perp}$ of the superlattice subband in the direction transverse to the stripe direction induces a broadening on the low density side of the resonance.

The decrease in the overdoped case $\rho < \rho_c$ is determined by the superlattice dispersion and the drop of the chemical potential toward the energy of the bottom of the 3rd subband. The width of the resonance and the drop in the underdoped regime $\rho > \rho_c$ is determined by the interaction cut off.

In Fig. 4(c) we report the variation of the chemical potential going from the superconducting to the normal phase. The relative variation of the chemical potential is usually negligible, less than 10^{-5}, in low T_c superconductors described by BCS theory with a nearly constant density of states. The variation is known to be large in a regime close to the Bose–Einstein condensation regime where all electrons of the system condense. Here the variation is of the order of 10^{-3} near the resonance and it can be understood because all electrons in the third subband condense. It is relevant that this important aspect of the superconducting phase shows a different behavior in the overdoped regime versus the underdoped regime with a change in sign of the variation of the chemical potential.

The T_c of the superconducting transition has been calculated by solving the linearized BCS equation by the iterative method

$$\Delta_n(k) = -\frac{1}{N}\sum_{n'k'} V_{nn'}(k,k')\frac{\mathrm{tgh}\left[(\xi_{n'}(k'))/2T_c\right]}{2\xi_{n'}(k')}\Delta_{n'}(k') \tag{7}$$

where $\xi_n(k) = \varepsilon_n(k) - \mu$.

The finite width of the stripes, the superlattice periodicity and quasi 2D subbands avoid strong fluctuations of the order parameter that destroy the 1D superconductivity.

We obtain the T_c for different values of the bulk effective coupling λ, defined as $\lambda = N_{n\to\infty}(\varepsilon_F)V_0$, where $N_{n\to\infty}(\varepsilon_F)$ is the DOS of a 2D free electron gas in a homogeneous plane. The T_c, for a bulk effective coupling $\lambda = 1/3$, is evaluated as a function of the electron charge density where the chemical potential is tuned above the bottom of the third subband. In Fig. 5 we report the results for different values of superlattice dispersion, $\Delta E_{3\perp}/\hbar\omega_0 = 0.8$ (panel a); 0.3 (panel b) and 0.15 (panel c) obtained by using an effective mass in the spacing material simulating the localized charges $m_b^* = 2.5$, 5 and 7.5, respectively.

The results show that the calculated shape of the resonance for the critical temperature is an asymmetric function of the charge density with respect to the critical value ρ_c giving a maximum in T_c and reproducing some general features of the curves of T_c versus doping in cuprates.

Another important characteristic of a superconducting system is the isotope effect. We have calculated the isotope coefficient for the superlattice of quantum stripes by estimating the variation of the T_c as a function of the isotopic mass M. The isotope coefficient is defined as $\alpha = -[\partial \ln(T_c)/\partial \ln(M)]$ assuming a mechanism driving to the superconducting instability where the cutoff energy for the interaction is connected with the isotopic mass of the lattice by $\hbar\omega_0 \propto M^{-1/2}$. so that $\alpha = 0.5[\partial \ln(T_c)/\partial \ln(\omega_0)]$.

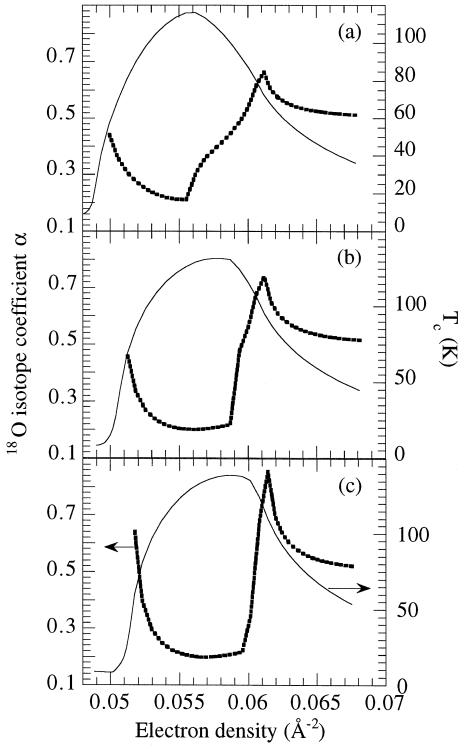

Fig. 5. The isotope coefficient and the superconducting critical temperature of the superlattice as a function of the electron charge density for different values of the transversal superlattice dispersion $\Delta E_{3\perp}/\hbar\omega_0 = 0.8$ (panel a); 0.3 (panel b) and 0.15 (panel c).

We have studied the isotope coefficient α as a function of the chemical potential and shown in Fig. 5. In the range where the critical temperature reaches the maximum we have found that the isotope coefficient has a small value with a minimum ($\alpha \approx 0.15$–0.2). This is due to the fact the energy cutoff $\hbar\omega_0$ is larger than the width of the singularity of the DOS at the resonance and all the electrons in the third subband form superconducting pairs and hence the T_c is weakly sensitive to small variations in the $\hbar\omega_0$. The isotope coefficient shows a maximum ($\alpha \approx 0.7$) at the edge of the shape resonance $|\mu - E_3| \sim \hbar\omega_0$ at $\rho = 0.06$ Å^{-2} as a small variation in the ω_0 could include or not the step increase of the DOS at the bottom of the subband. As can be seen in the $\alpha(\rho)$ curve, it takes asymmetric shape with respect to the minimum value. The energy width of the flat region where α has a small value is of the order of $\hbar\omega_0$. The $T_c(\rho)$ phase diagram and the isotope coefficient $\alpha(\rho)$ give experimental constraints on the value of the characteristic energy cutoff $\hbar\omega_0$ for the effective interaction. It should be mentioned that the width of the drop of the isotope coefficient from 0.7 to 0.15 is controlled by the dispersion of the superlattice subband $\Delta E_{3\perp}$.

The pronounced spikes in α follow from the sharp BCS energy cutoff $\hbar\omega_0$ in the attractive interaction. In the strong coupling Eliashberg theory the inclusion of dynamic and self energy corrections are expected to get away the sharp cutoff and hence smooth the spikes.

In Fig. 6 we report the variation of the maximum values of the critical temperature reached at the resonance $T_{c\max}$ as a function of the effective coupling λ for the different cases of superlattice dispersion considered in Fig. 5. The values of $T_{c\max}$ in the superlattice obtained by tuning the stripe width and the charge density are compared with the critical temperature of the homogenous plane formed by the same electron gas in the superconducting stripes $T_{c\infty}$. We show that while the critical temperature in the homogeneous plane changes

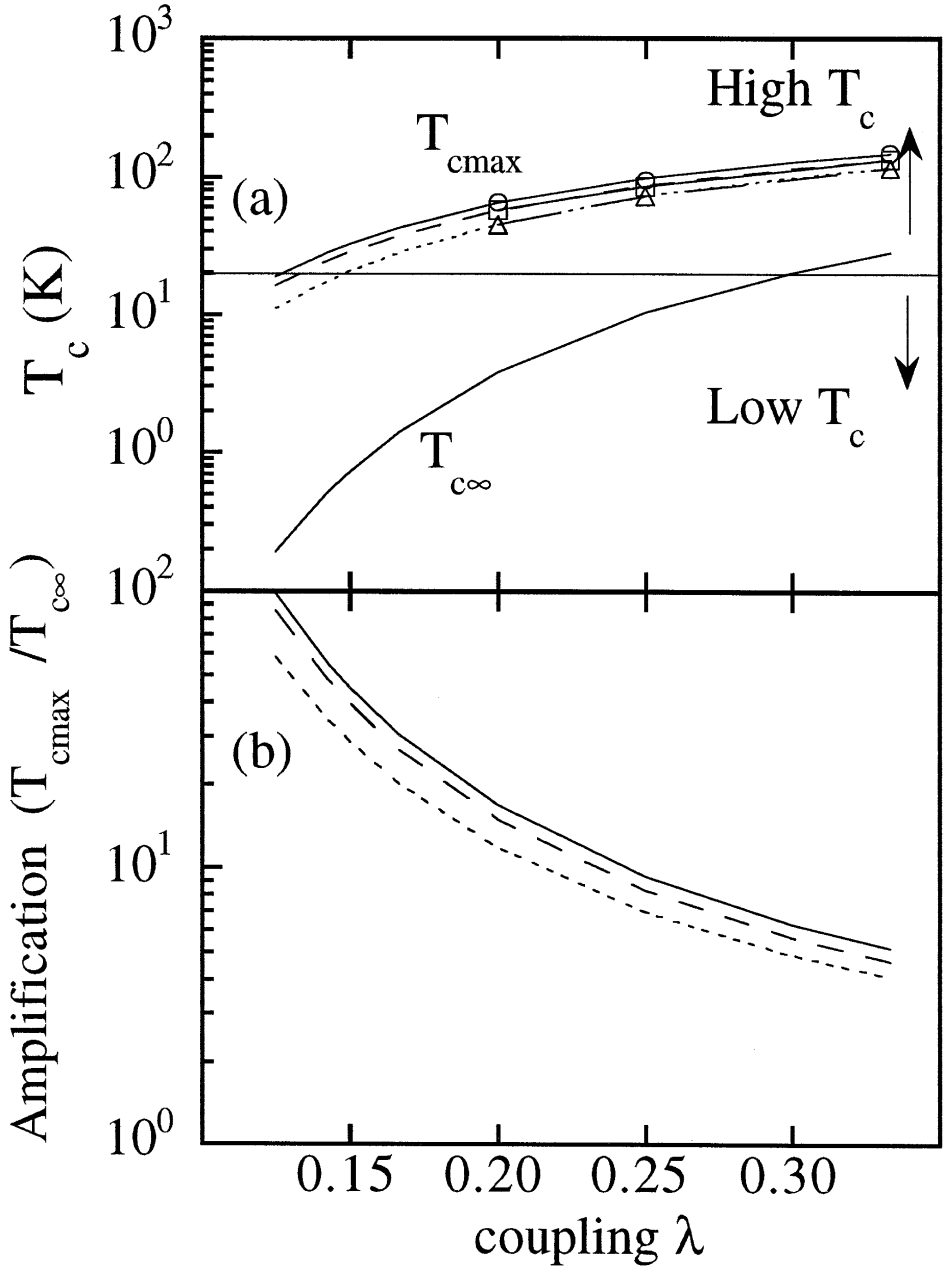

Fig. 6. (a) The critical temperature reached at the maximum of the resonance $T_{c\,max}$ as a function of the effective coupling λ for the different cases of superlattice dispersion $\Delta E_{3\perp}/\hbar\omega_0 = 0.8$ (dotted line); 0.3 (dashed line) and 0.15 (solid line); and the critical temperature of the homogenous plane $T_{c\infty}$. (b) The value of the T_c amplification due to the superlattice topology as function of the effective coupling.

from 0.01 to 20 K by increasing the effective coupling λ in this range, as in all 3D superconducting metals and alloys, in the superlattice the critical temperature is in the high-T_c range 20 K $< T_c <$ 120 K typical of cuprate superconductors.

4. Discussion

High-T_c superconductors show anomalous normal state properties with two different phases: an underdoped and an overdoped regime separated by optimum doping that gives the highest superconducting critical temperature. The particular superconducting phase described above has many similarities with the high-T_c phase of doped cuprate perovskites. In fact the universal curves of T_c versus doping for all families of cuprate superconductors show a resonance behavior of T_c versus charge density. We have plotted the experimental values of T_c [41–43] and of the isotope coefficient in $La_{2-x}Sr_xCuO_4$ [33,34] as function of charge density in Fig. 7. The surface electron number density is given by $\rho = (1-\delta)/3.8^2$ in $Å^{-2}$ where δ is the doping, i.e., the number of holes per Cu site.

The superconducting striped phase is expected to be formed at the metal to insulator transition at about $\rho_{MIT} = 0.065$ $Å^{-2}$ and disappears at high doping at about $\rho = 0.052$ $Å^{-2}$. In this regime the period of the superlattice due to charge ordering shows a large variation with doping in the underdoped regime but it is nearly constant at optimum doping and in the overdoped regime [24,25]. The agreement of the experimental data with the calculations of T_c and the isotope coefficient in Fig. 5(b) are very interesting. The agreement indicates that the natural superlattice of quantum stripes is stable in the resonance range. The actual value of the calculated critical temperature is larger than in the experiments in LaSrCu but it can decrease with decreasing the coupling and it is expected to decrease by self energy corrections.

The anomalous features of the normal phase in the underdoped regime (1) the linear behavior of resistivity; (2) the trend toward charge localization for T close to zero when superconductivity is quenched by a high magnetic field [44]; and (3) the opening of a pseudogap at the Fermi surface [37] can be understood in the frame of the present calculations with the quasi 1D character of the electronic structure in the underdoped regime.

On the other hand, the 2D-like behavior in the overdoped regime is indicated (1) by the divergence of the resistivity from the linear behavior [42]; and (2) by the closing of the pseudogap of the Fermi surface [37] observed experimentally.

The characteristic behavior of the isotope coefficient and the large variation of the chemical potentials going from the normal to the superconducting phase [45] show that it is possible that the origin of the T_c amplification in the cuprate has its basis on a mesoscopic structure made of quantum stripes. These results support the assignment of the anomalous properties of the normal and superconducting phase in doped cuprate superconductors to a natural segregation of a localized and delocalized charge that forms a natural superlattice of quantum stripes in a crossover regime between a low doped antiferromagnetic phase and normal 2D metallic phase at high hole densities.

Our calculation of T_c and of the electronic structure can be improved by overcoming several first order approximations that have been made here such as the use of a free electron model for the electronic structure

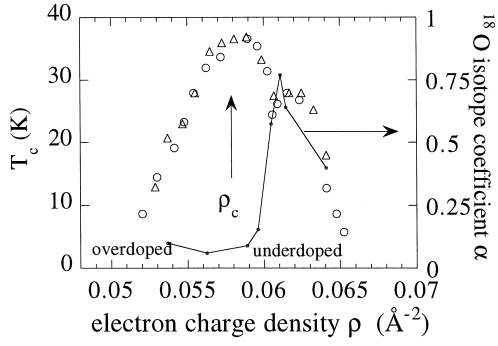

Fig. 7. The superconducting critical temperature of $La_{2-x}Sr_xCuO_4$ from Ref. [41] (circles) and Ref. [43] (triangles) and the isotope coefficient [31] versus the surface charge number density $\rho = (1-\delta)/3.8^2$, where δ is the doping or the number of holes per Cu site.

and the assumption of an isotropic s-wave pairing, and taking into account dynamic and self energy corrections within Eliashberg theory and vertex corrections [46]. These improvements of the theoretical calculations have to be done, however, we think that they will not change the basic physical features of the amplification of the critical temperature and the peculiar behavior of the isotope effect described here.

By using this mechanism for the T_c amplification it is possible to produce new heterostructures made of superlattices of quantum wires with a critical temperature higher than that of the homogeneous bulk materials, and it will be possible to overcome the present record for the critical temperature of 150 K and to approach room temperature.

Acknowledgements

This work was partially funded by Consiglio Nazionale delle Ricerche, Istituto Nazionale di Fisica della Materia, and Istituto Nazionale di Fisica Nucleare.

References

[1] J.G. Bednorz, K.A. Müller, Rev. Mod. Phys. 60 (1988) 565.
[2] J.-M. Triscone, D. Fiscer, O. Brunner, L. Antognazza, A.D. Kent, M.G. Karkut, Phys. Rev. Lett. 64 (1990) 804.
[3] Q. Li, X.X. Xi, X.D. Wu, A. Inam, S. Vadlamannati, W.L. McLean, T. Venkatesan, R. Ramesh, D.M. Hwang, J.A. Martinez, L. Nazar, Phys. Rev. Lett. 64 (1990) 3086.
[4] R. Fastampa, M. Giura, R. Marcon, E. Silva, Phys. Rev. Lett. 67 (1991) 1795.
[5] I. Bosovic, J.N. Eckstein, M.E. Klausmeier-Brown, G. Virshup, J. Supercond. 5 (1992) 19.
[6] P. Müller, in: R. Helbig (Ed.), Festkörperprobleme/Advances in Solid State Physics 34, Vieweg, Braunschwig, 1994, p. 1.
[7] S.T. Ruggiero, M.P. Beasley, in: L.L. Chang, B.C. Giessen (Eds.), Synthetic Modulated Structures, Academic Press, New York, 1985, p. 365.
[8] B.Y. Jin, J.B. Ketterson, Adv. Phys. 38 (1989) 189.
[9] J.B. Goodenough, J.S. Zhou, Nature 386 (1997) 229.
[10] A. Bianconi, M. Missori, J. Phys. I (France) 4 (1994) 361.
[11] A. Bianconi, M. Missori, H. Oyanagi, H. Yamaguchi, D.H. Ha, Y. Nishiara, S. Della Longa, Europhys. Lett. 31 (1995) 411.
[12] A. Bianconi, M. Lusignoli, N.L. Saini, P. Bordet, Å. Kvick, P.G. Radaelli, Phys. Rev. B 54 (1996) 4310.
[13] A. Bianconi, N.L. Saini, T. Rossetti, A. Lanzara, A. Perali, M. Missori, H. Oyanagi, H. Yamaguchi, Y. Nishihara, D.H. Ha, Phys. Rev. B 54 (1996) 12018.
[14] A. Lanzara, N.L. Saini, A. Bianconi, J.L. Hazemann, Y. Soldo, F.C. Chou, D.C. Johnston, Phys. Rev. B 55 (1997) 9120.
[15] B.W. Statt, P.C. Hammel, Z. Fisk, S.-W. Cheong, F.C. Chou, D.C. Johnston, J.E. Schirber, Phys. Rev. B 52 (1995) 15575.
[16] A. Bianconi, N.L. Saini, A. Lanzara, M. Missori, T. Rossetti, H. Oyanagi, H. Yamaguchi, K. Oka, T. Ito, Phys. Rev. Lett. 76 (1996) 3412.
[17] Proc. Int. Conf. 'Stripes and Lattice Instabilities and High-T_c Superconductivity', Roma, 8–13 December, 1996; A. Bianconi, N.L. Saini (Eds.), J. Supercond. 10 (4) (1977) special issue.
[18] A. Bianconi, in: S.K. Joshi C.N.R. Rao, S.V. Subramanyam (Eds.), International Conference on Superconductivity, Bangalore, January 10–14, 1990, World Scientific Singapore, 1990, p. 448.
[19] A. Bianconi, A.M. Flank, P. Lagarde, C. Li, I. Pettiti, M. Pompa, D. Udron, in: J. Ashkenazi, S.E. Barnes, F. Zuo, G.C. Vezzoli, B.M. Klein (Eds.), High-Temperature Superconductivity, Plenum Press, New York, 1991, p. 363.
[20] A. Bianconi, S. Della Longa, M. Missori, I. Pettiti, M. Pompa, in: Y. Bar-Yam, T. Egami, J. Mustre de Leon, A.R. Bishop (Eds.), Lattice Effects in High-T_c Superconductors, Proc. Meeting in Santa Fe, New Mexico, January 13–15, 1992, World Scientific, Singapore, 1992, p. 95.
[21] A. Bianconi, in: K.A. Muller, G. Benedek (Ed.), Phase Separation in Cuprate Superconductors, Proc. of the Erice Workshop, May 6–12, 1992, World Scientific, Singapore, 1993, p. 125.
[22] A. Bianconi, S. Della Longa, M. Missori, I. Pettiti, M. Pompa, A. Soldatov, Jpn. J. Appl. Phys. 32 (suppl. 32-3) (1993) 578–580.
[23] A. Bianconi, Physica C 235–240 (1994) 269.
[24] A. Bianconi, Solid State Commun. 91 (1994) 1.
[25] A. Bianconi, M. Missori, Solid State Commun. 91 (1994) 287.
[26] Y. Guo-meng, M.B. Hunt, H. Keller, K.A. Müller, Nature 385 (1997) 236.

[27] F. Borsa, P. Carretta, J.H. Cho, F.C. Chou, Q. Hu, D.C. Johnston, A. Lascialfari, D.R. Torgeson, R.J. Gooding, N.M. Salem, J.E. Vos, Phys. Rev. B 52 (1995) 7334.
[28] J.M. De Teresa, M.R. Ibarra, P.A. Algarabel, C. Ritter, C. Marquina, J. Blasco, J. Garcia, A. del Moral, Z. Arnold, Nature 386 (1997) 256.
[29] T. Egami, D. Louca, R.J. McQueeney, J. Supercond. 10 (1977) 323.
[30] A. Bianconi, Solid State Commun. 89 (1994) 933.
[31] A. Perali, A. Bianconi, A. Lanzara, N.L. Saini, Solid State Commun. 100 (1996) 181.
[32] A. Bianconi, A. Valletta, A. Perali, N.L. Saini, Solid State Commun. 102 (1997) 369.
[33] M.K. Crawford, M.N. Kunchur, W.E. Farneth, E.M. McCarron III, S.J. Poon, Phys. Rev. B 41 (1) (1990) 282.
[34] M.K. Crawford, W.E. Farneth, E.M. McCarron III, R.L. Harlow, A.H. Moudden, Science 250 (1990) 1390.
[35] D. Zech, H. Keller, K. Conder, E. Kaldis, E. Liarokapis, N. Poulakis, K.A. Müller, Nature 371 (1994) 681.
[36] J. Ma, P. Almeras, R.J. Kelley, H. Berger, G. Magaritondo, X.Y. Cai, Y. Feng, M. Onellion, Phys. Rev. B 51 (1995) 9271.
[37] H. Ding, T. Yokoya, J.C. Campuzano, T. Takahashi, M. Randeria, M.R. Norman, T. Mochiku, K. Kadowaki, J. Giapintzaki, Nature 382 (1996) 51.
[38] A.G. Loeser, Z.X. Shen, D.S. Dessau, D.S. Marshall, C.H. Park, P. Fournier, A. Kapitulnik, Science 273 (1996) 325.
[39] J.M. Harris, Z.-X. Shen, P.J. White, D.S. Marshall, M.C. Schabel, J.N. Eckstein, I. Bozovic, Phys. Rev. B 54 (1996) 15665.
[40] N.L. Saini, J. Avila, A. Bianconi, A. Lanzara, M.C. Asensio, S. Tajima, G.D. Gu, N. Koshizuka, Phys. Rev. Lett. 79 (1997) 3467.
[41] H. Takagi, T. Ido, S. Ishibashi, M. Uota, S. Uchida, Y. Tokura, Phys. Rev. B 40 (1989) 2254.
[42] H. Takagi, R.J. Cava, M. Marezio, B. Battlog, J.J. Krajezski, W.F. Peck Jr., Phys. Rev. Lett. 68 (1992) 3777.
[43] P.G. Radaelli, D.G. Hinks, A.W. Mitchell, B.A. Hunter, J.L. Wagner, B. Dabrowski, K.G. Vandervoort, H.K. Viswanathan, J.D. Jorgensen, Phys. Rev. B 49 (1994) 4163.
[44] G.S. Boebinger, Y. Ando, A. Passner, T. Kimura, M. Okuya, J. Shimoyama, K. Kishio, K. Tamasaku, N. Ichikawa, S. Uchida, Phys. Rev. Lett. 77 (1996) 5417.
[45] G. Rietveld, N.Y. Chen, D. van der Marel, Phys. Rev. Lett. 69 (1992) 2578.
[46] L. Pietronero, G. Grimaldi, S. Strässler, Phys. Rev. Lett. 75 (1995) 1158.